Supporting Information

Quantitative Prediction of the Structure and Viscosity of Aqueous Micellar Solutions of Ionic Surfactants: A Combined Approach Based on Coarse-grained MARTINI Simulations Followed by Reverse-mapped All-atom Molecular Dynamics Simulations

Stavros D. Peroukidis,[1,2] Dimitrios G. Tsalikis,[1] Massimo G. Noro,[3] Ian P. Stott,[4] and Vlasis G. Mavrantzas[1,5]

[1]Department of Chemical Engineering, University of Patras and FORTH-ICE/HT, GR 26504, Patras, Greece

[2]Hellenic Open University, Patras GR 26222, Greece

[3]UKRI Science and Technology Facilities Council, Daresbury, WA4 4AD, UK

[4]Unilever Research & Development Port Sunlight, Bebington CH63 3JW, UK

[5]ETH Zürich, Department of Mechanical and Process Engineering, Particle Technology Laboratory, CH-8092 Zürich, Switzerland

1. The standard and the modified MARTINI Force Fields, and the corresponding MD simulations

In the original or standard MARTINI[1] force field (FF), each SDS molecule consists of three tail (C_1) beads and a sulfate (OSO_3) group or head (Q_a) bead; the latter is also assigned a charge of -1 e. In addition, the model makes use of water (W or P4) beads each one of which represents four water molecules and of hydrated sodium ions (Na or Q_d) with a charge of +1 e playing the role of counterbalance ions. Hydrated chloride ions (Cl or Q_a) with a charge of -1 e are also assumed when salt (e.g., NaCl) is also present in the formulation.

Bonded interactions in the MARTINI FF are modelled through a bond-stretching potential for all pairs of chemically-bonded beads and a bond angle-bending potential for any two beads along the molecule separated by two bonds. The functional form of these two potentials and their parametrization are reported in Table S1. Non-bonded interactions, on the other hand, are modelled through a standard 12-6 Lennard-Jones (LJ) potential and an electrostatic (Coulomb) potential. LJ interactions between neighboring sites up to three bonds apart (i.e., 1-4 interactions) are not considered. In an MD simulation with the MARTINI FF, the LJ potential is truncated at r_{cut} = 13 Å. Then, for the LJ energy and the corresponding force to drop smoothly to zero at r_{cut}, a cubic spline interpolation is utilized for distances between r_{sp} = 10 Å and r_{cut}. The functional form and the parameter values of the terms describing non-bonded interactions in MARTINI are reported in Table S2.

Optimal values for the relative permittivity ε_r and the sigma parameter, σ_{C_1,C_1}, of the LJ interaction for tail beads (the LJ C_1-C_1 interaction) were obtained by trial-and-error, by running several test MD simulations (each for about 200 ns) with a system comprising 375 SDS molecules at total surfactant concentration $c_T \approx$ 180 mM (Table S3). The optimal values were obtained by looking

at the mean aggregation number for the system under study and comparing it with the corresponding experimentally known value. Relatively large values of ε_r (e.g., close to 40) were observed to result in relatively small mean aggregation numbers whereas smaller values of ε_r were observed to result in unrealistically large aggregates.

In our study, the coarse-grained (CG) molecular dynamics (MD) simulations with the standard MARTINI FF were performed in the isothermal-isobaric (NPT) statistical ensemble at temperature T = 300 K and pressure P = 1 atm using the GROMACS[2-4] software. The temperature and the pressure were constrained at their prescribed values using the Berendsen thermostat and barostat,[5] respectively. The velocity-Verlet algorithm was employed to integrate Newton's equations of motion using an integration time step equal to dt = 20 fs. Large cubic simulation cells (subject to periodic boundary conditions) were employed comprising several hundreds of SDS molecules and hundreds of thousands of interacting beads in total (due to the presence of water molecules) to ensure the absence of any finite system size effects and reduce the statistical uncertainty of the properties computed. In Table S4 we report some additional technical details concerning the systems generated and simulated with the modified MARTINI FF.

Table S1. Values of the MARTINI FF[1] parameters defining the bond-stretching and the bond angle-bending potential energy functions.

Bond stretching	$U_{str}(r) = \frac{k_{str}}{2}(r - r_0)^2$	
	r_0 (Å)	k_{str} (kJ/nm^2)

C_1—SO_3	4.04	20,000
C_1—C_1	4.7	20,000
Bond bending	$U_{\text{bend}}(\theta) = \frac{k_{\text{bend}}}{2}\left[\cos(\theta) - \cos(\theta_0)\right]^2$	
	θ_0 (degrees)	k_{bend} (kJ/mol)
SO_3—C_1—C_1	170	15
C_1—C_1—C_1	180	25

Table S2. Values of the MARTINI FF[1] parameters defining the non-bonded Lennard-Jones (LJ) and electrostatic (Coulomb) potential energy functions. In the modified version of the MARTINI FF, the parametrization of the C_1—C_1 LJ interaction was changed; the new values are shown in parenthesis.

Lennard-Jones	$U_{\text{LJ}}(r_{ij}) = 4\varepsilon_{\text{ij}}\left[\left(\frac{\sigma_{\text{ij}}}{r_{\text{ij}}}\right)^{12} - \left(\frac{\sigma_{\text{ij}}}{r_{\text{ij}}}\right)^{6}\right]$	
	$4\varepsilon_{\text{ij}}\sigma_{\text{ij}}^6$ (kJ nm^6/mol)	$4\varepsilon_{\text{ij}}\sigma_{\text{ij}}^{12}$ (kJ nm^{12}/mol)
OSO_3—OSO_3	0.21558	0.0023238
OSO_3—C_1	0.45440	0.025810
OSO_3—W	0.24145	0.0026027
OSO_3—HW	0.24145	0.0026027
OSO_3—Na	0.24145	0.0026027
OSO_3—C_1	0.21558	0.0023238
C_1—C_1	0.15091 (0.38753)	0.0016267 (0.010727)
C_1—H	0.086233	0.92953×10^{-3}
C_1—HW	0.086233	0.92953×10^{-3}
C_1—Na	0.45440	0.025810
C_1—Cl	0.45440	0.025810
H—HW	0.21558	0.0023238
H—HW	0.76824	0.026348
H—Na	0.24145	0.0026027

H—Cl	0.24145	0.0026027
HW—HW	0.21558	0.0023238
HW—Na	0.24145	0.0026027
HW—Cl	0.24145	0.0026027
Na—Na	0.21558	0.0023238
Na—Cl	0.24145	0.0026027
Cl—Cl	0.21558	0.23238

Coulomb	$U_{\mathrm{Coul}}\left(r_{\mathrm{ij}}\right)=\frac{q_{\mathrm{i}}q_{\mathrm{j}}}{4\pi\varepsilon_0\varepsilon_{\mathrm{r}}r_{\mathrm{ij}}}$
	q (e)
OSO3 (Q_a)	-1
C_1	0
W (P4)	0
HW (BP4)	0
Na (Q_d)	+1
Cl (Q_a)	-1

Table S3. Optimal values of the relative permittivity ε_{r} and of the sigma LJ parameter for the C_1—C_1 interaction (σ_{C_1,C_1}, in nm) based on the comparison of predicted mean aggregation numbers with experimentally reported data.

σ_{C_1,C_1} (nm) / ε_{r}	**0.6**	**0.55**	**0.5**
20	180	190	-
30	35	**53**	27.5
40	25	25	-

Table S4. Additional simulation details regarding the CG MD simulations with the original and the modified MARTINI FF.

System	Number of SDS molecules	Number of water (W) beads	Number of Hydrated sodium ion (Na) beads	Total number of beads	T (K)	c_T (mM)
1	625	164826	625	167951	300	52
2	1080	146773	1080	152173	300	100
3	1296	121816	1296	128296	300	142
4	1715	120296	1715	128871	300	185
5	2560	131940	2560	144740	300	247

2. Aggregation number distributions from the Coarse–Grained model

Results from the CG MD simulations with the modified MARTINI FF for the distribution $P(k)$ of the aggregation number k of surfactants per micelle for various surfactant concentrations c_T are presented in Figure S1. The histograms of Figure S1 have been calculated by averaging over all configurations accumulated in the last 0.5 μs of the trajectory. In all cases, we see that the $P(k)$-vs.-k plots are made of two parts which are separated by a local minimum: the part on the left of the local minimum reflects the $P(k)$ values that correspond to monomers, dimers, etc. comprising the so called sub-micellar region of the graph; the values of $P(k)$ in this part of the graph decrease with increasing value of k. On the other hand, the part of the graph on the right hand side of the minimum reflects the $P(k)$ values that correspond to larger micelles in the solution, comprising the so called micellar region of the graph.

The sub-micellar part of the $P(k)$-vs.-k graph allows one to obtain also a rough estimate of the so-called "free" surfactant concentration c_F defined as the total number of SDS molecules that belong to this part of the graph divided by the average volume of the system. The simplest method[6] to estimate the first CMC is from the plateau value of the c_F-vs.-c_T plot shown in Figure S2. This results in a critical micelle concentration CMC from the CG MD simulations approximately equal to 5 mM. This CMC value is in favourable agreement with the experimentally known value for SDS,[7] which is 8 mM. More elaborate methods to calculate the first CMC are discussed in ref 6 but their implementation here exceeds the scope of the present work.

The micellar part of the $P(k)$-vs.-k plot, on the other hand, allows one to calculate the mean aggregation number $\langle k \rangle = \frac{N_{\text{total}}}{N_{\text{micelles}}} \sum_{k=N_{\text{min}}}^{N_{\text{total}}} k \cdot P(k)$, where N_{total} is the total number of SDS molecules in the simulation cell, N_{min} the value of k for which $P(k)$ exhibits its local minimum and N_{micelles} the total number of SDS molecules belonging to micelles having k values larger than N_{min}. Here, we set empirically N_{min} = 15, implying that an aggregate formed in the simulation cell is considered as a true micelle only if it contains at least 15 SDS molecules.

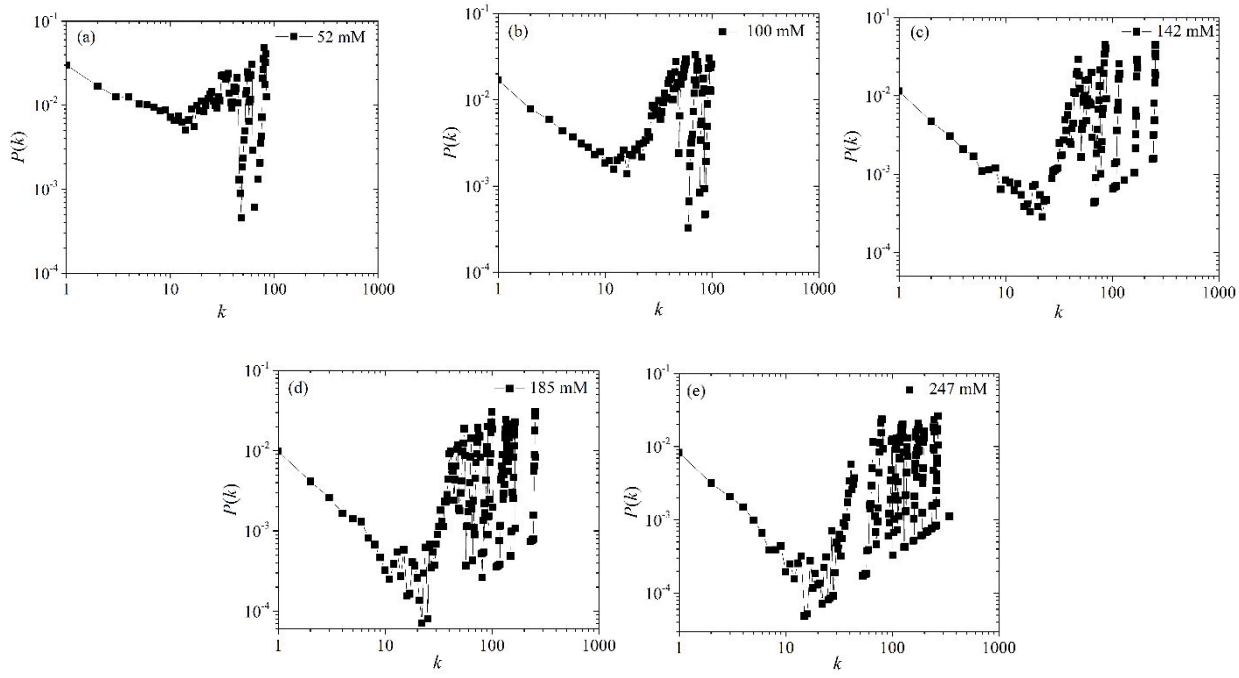

Figure S1. Simulation predictions with the modified MARTINI FF for the distribution $P(k)$ of the aggregation number k of surfactants per micelle and its dependence on total SDS concentration c_T: (a) 52 mM, (b) 100 mM, (c) 142 mM, (d) 185 mM, and (e) 247 mM.

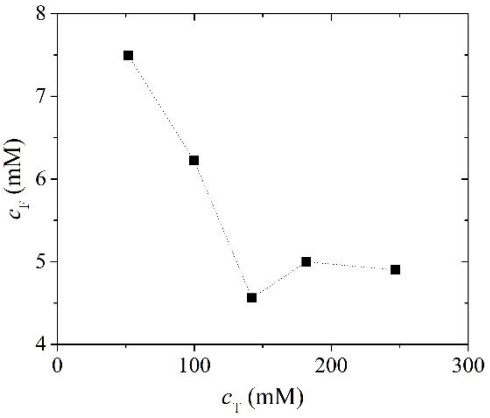

Figure S2. Dependence of the free SDS surfactant concentration c_F on the total SDS surfactant concentration c_T. Results from the present CG MD simulations with the modified MARTINI FF.

3. Time evolution of the mean aggregation number in the course of the Coarse-Grained MD simulations

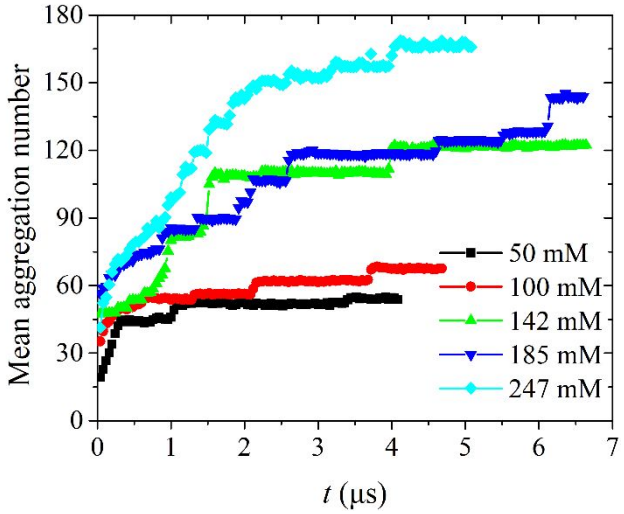

Figure S3. Time evolution of the mean aggregation number $\langle k \rangle$ in the course of the CG MD simulations with the modified MARTINI FF as a function of total surfactant concentration c_T. In all cases, the curves present a very similar pattern: the mean aggregation number increases with time, but with a constantly decreasing rate implying the attainment of a plateau at long times.

4. The relative shape anisotropy parameter (asphericity parameter) in the case of the Coarse-Grained model

To detect changes in the shape of the micelles formed in the course of the CG MD simulations with increasing total surfactant concentration c_T (experimentally, as the concentration of the surfactant increase, the shape of the micelles changes from spherical to rod-like), we computed the so called relative shape anisotropy parameter A.[8, 9] The calculation of A is based on the calculation of the radius-of-gyration matrix **S** for each micelle in the solution. If λ_1, λ_2, and λ_3 are the three

eigenvalues of the matrix **S**, then the relative shape anisotropy parameter is defined as

$$A=1-3\frac{\lambda_1\lambda_2+\lambda_1\lambda_3+\lambda_2\lambda_3}{R_g^4}$$ or, equivalently, $$A=\frac{\left(\lambda_1^2-\lambda_2^2\right)^2+\left(\lambda_2^2-\lambda_3^2\right)^2+\left(\lambda_1^2-\lambda_3^2\right)^2}{4R_g^4}$$ where

$R_g^2=\lambda_1+\lambda_2+\lambda_3$. Values of A close to 0 point out to a spherical micelle whereas values of A close to 1 point out to a rod-like micelle.

In Figure S4 we report our CG MD simulation predictions with the modified MARTINI FF for the distribution function $P(A)$ of the relative shape anisotropy parameter A and how it varies with the total surfactant concentration c_T.

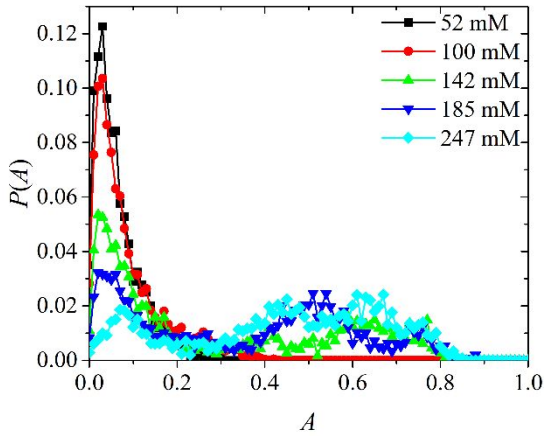

Figure S4. Normalized distribution of the relative shape anisotropy parameter A.

5. Simulation details for the reverse-mapped AA MD simulation cells

Table S5. Simulation details for the reverse-mapped AA MD simulation cells.

System	Number of SDS molecules	Number of Water molecules	SDS concentration, $C_{SDS}(c_T)$ (mM)	Number of Na^+ ions
1	625	650264	53	625
2	1080	575923	103	1080
3	1296	487264	145	1296
4	1715	480285	192	1715
5	2560	527760	257	2560

6. Aggregation number distributions from the AA MD simulations

Distribution functions $P(k)$ of the mean aggregation number $\langle k \rangle$ of surfactants per micelle obtained from the AA MD simulations for various surfactant concentrations c_T are displayed in Figure S5. They have been computed by averaging over configurations accumulated during the last 4 ns of the output trajectory. The $\langle k \rangle$ from the AA simulations is computed through $\langle k \rangle = \frac{N_{total}}{N_{micelles}} \sum_{k=N_{min}}^{N_{total}} k \cdot P(k)$ where N_{total} denotes the total number of SDS molecules in the simulation cell and $N_{min} = 15$ (implying that an aggregate is considered as a micelle if it consists of more than 15 SDS molecules).

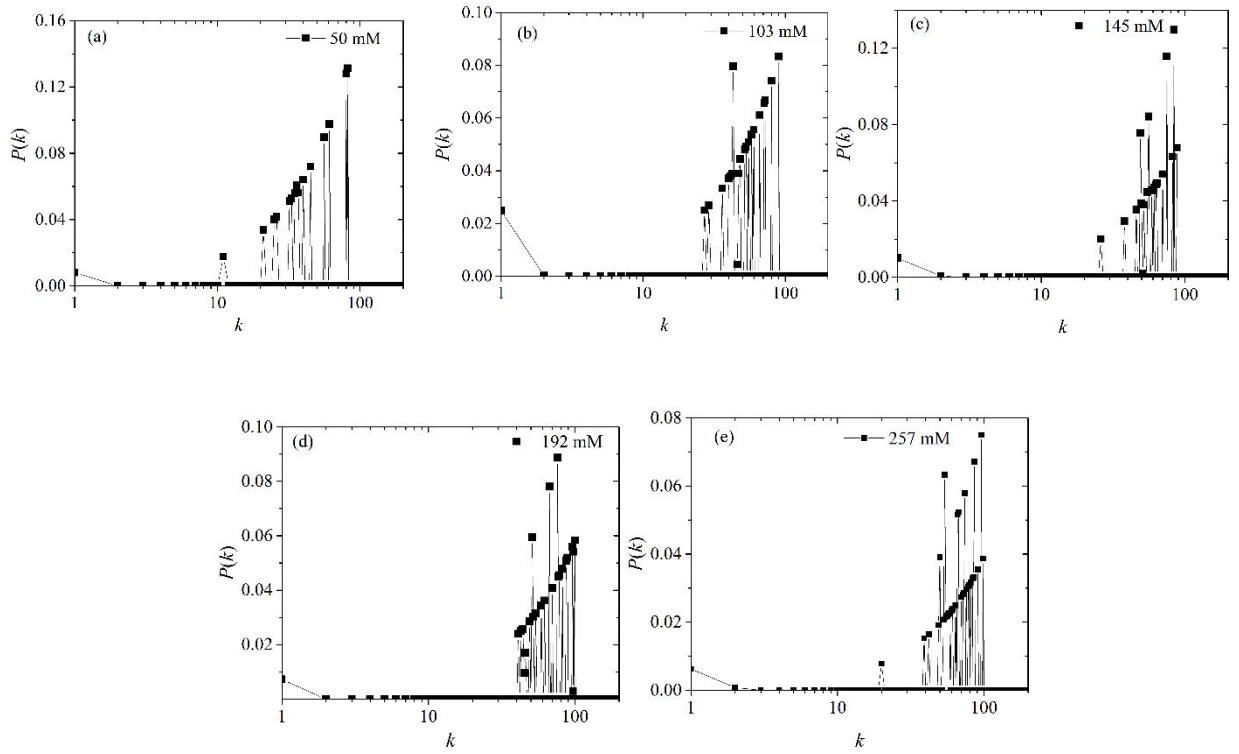

Figure S5. Distributions $P(k)$ of the aggregation number k of surfactants per micelle for different SDS concentrations c_T: (a) 53 mM, (b) 103 mM, (c) 145 mM, (d) 192 mM, and (e) 257 mM.

References

1. Marrink, S. J.; Risselada, H. J.; Yefimov, S.; Tieleman, D. P.; de Vries, A. H. The MARTINI force field: Coarse grained model for biomolecular simulations. *J. Phys. Chem. B* **2007,** *111* (27), 7812-7824.
2. Berendsen, H. J. C.; Van der Spoel, D.; Vandrunen, R. GROMACS: A message-passing parallel molecular dynamics implementation. *Comput. Phys. Commun.* **1995,** *91* (1-3), 43-56.
3. Hess, B.; Kutzner, C.; van der Spoel, D.; Lindahl, E. GROMACS 4: Algorithms for highly efficient, load-balanced, and scalable molecular simulation. *J. Chem. Theory Comput.* **2008,** *4* (3), 435-447.
4. Van der Spoel, D.; Lindahl, E.; Hess, B.; Groenhof, G.; Mark, A. E.; Berendsen, H. J. C. GROMACS: Fast, flexible, and free. *J. Comput. Chem.* **2005,** *26* (16), 1701-1718.
5. Berendesen, H. J. C.; Postma, J. P. M.; DiNola, A.; Haak, J. R. Molecular dynamics with coupling to an external bath. *J. Chem. Phys.* **1984,** *81* (8), 3684-3690.
6. Anderson, R. L.; Bray, D. J.; Del Regno, A.; Seaton, M. A.; Ferrante, A. S.; Warren, P. B. Micelle formation in alkyl sulfate surfactants using dissipative particle dynamics. *J. Chem. Theory Comput.* **2018,** *14* (5), 2633-2643.

7. Anachkov, S. E.; Danov, K. D.; Basheva, E. S.; Kralchevsky, P. A.; Ananthapadmanabhan, K. P. Determination of the aggregation number and charge of ionic surfactant micelles from the stepwise thinning of foam films. *Adv. Colloid Interface Sci.* **2012,** *183-184*, 55-67.
8. Arkin, H.; Janke, W. Gyration tensor based analysis of the shapes of polymer chains in an attractive spherical cage. *J. Chem. Phys.* **2013,** *138* (5), 054904.
9. Theodorou, D. N.; Suter, U. W. Shape of unperturbed linear polymers. Polypropylene. *Macromolecules* **1985,** *18* (6), 1206-1214.